References

1. Giddings, J. C. *Science* **1993**, *260*, 1456.
2. Giddings, J. C. *Chem. Eng. News* **1988**, *66*, 34.
3. Caldwell, K. D. *Anal. Chem.* **1988**, *60*, 959A.
4. Martin, M.; Williams, P. S. In *Theoretical Advancement in Chromatography and Related Separation Techniques*; *NATO ASI Series C Mathematical and Physical Sciences*; Dondi. F.; Guiochon, G. Eds.; Kluwer: Dordrecht, 1992; Vol. 383, p 513.
5. Giddings, J. C.; Yang, F. J. F.; Myers, M. N. *Anal. Chem.* **1974**, *46*, 1917.
6. Giddings, J. C.; Ratanathanawongs, S. K.; Moon, M. H. *KONA: Powder and Particle* **1991**, *9*, 200.
7. Myers, M. N.; Caldwell, K. D.; Giddings, J. C. *Sep. Sci. Technol.* **1974**, *9*, 47.
8. Giddings, J. C.; Hovingh, M. E.; Thomson, G. H. *J. Phys. Chem.* **1970**, *74*, 4291.
9. Caldwell, K. D.; Kesner, L. F.; Myers, M. N.; Giddings, J. C. *Science* **1972**, *176*, 296.
10. Giddings, J. C.; Yang, F. J. F.; Myers, M. N. *Science* **1976**, *193*, 1244.
11. Moon, M. H.; Giddings, J. C. *J. Pharm. Biomed. Anal.* **1993**, *11*, 911.
12. Litzen, A.; Wahlund, K.-G. *J. Chromatogr.* **1989**, *476*, 413.
13. Liu, M. K.; Li, P.; Giddings, J. C. *Protein Science* **1993**, *2*, 1520.
14. Giddings, J. C.; Benincasa, M. A.; Liu, M. K.; Li, P. *J. Liq. Chromatogr.* **1992**, *27*, 1489.
15. Hansen, M. E.; Giddings, J. C. *Anal. Chem.* **1989**, *61*, 811.
16. Moon, M. H.; Williams, P. S.; Giddings, J. C. Unpublished results.
17. Giddings, J. C.; Yang, F. J. F.; Myers, M. N. *Anal. Chem.* **1976**, *48*, 1126.
18. Giddings, J. C.; Williams, P. S.; Benincasa, M. A. *J. Chromatogr.* **1992**, *627*, 23.

Mechanistic Studies on the Oxidation of Triphenylphosphine by $[(tpy)(bpy)Ru^{IV}=O]^{2+}$, Structure of the Parent Complex $[(tpy)(bpy)Ru^{II}\text{-}OH_2]^{2+}$

Won Kyung Seok*[†], Mee Yung Kim[†], Yoshinobu Yokomori[‡],
Derek J. Hodgson[++], and Thomas J. Meyer*[§]

[†] *Department of Chemistry, Dongguk University, Seoul 100-715, Korea*
[‡] *Department of Chemistry, The National Defence Academy, Hashirimizu, Yokosuka 239, Japan*
[++] *Department of Chemistry, University of Wyoming, Laramie, Wyoming 82071, U.S.A.*
[§] *Department of Chemistry, The University of North Carolina at Chapel Hill, Chapel Hill, NC 27599-3290, U.S.A.*

Received March 23, 1995

Oxidation of triphenylphosphine to triphenylphosphine oxide by $[(tpy)(bpy)Ru(O)]^{2+}$ (tpy is 2,2′ : 6′,2″-terpyridine and bpy is 2,2′-bipyridine) in CH_3CN has been studied. Experiments with the ^{18}O-labeled oxo complex show that transfer of oxygen from $[(tpy)(bpy)Ru^{IV}=O]^{2+}$ to triphenylphosphine is quantitative within experimental error. The reaction is first order in each reactant with k (25.3 ℃)$=1.25\times10^6$ $M^{-1}s^{-1}$. The inital product, $[(tpy)(bpy)Ru^{II}\text{-}OPPh_3]^{2+}$, is formed as an observable intermediate and undergoes slow k (25 ℃)$=6.7\times10^{-5}$ s^{-1} solvolysis. Activation parameters for the oxidation step are $\Delta H^{\neq}=3.5$ kcal/mol and $\Delta S^{\neq}=-23$ eu. The geometry at ruthenium in the complex cation, $[(tpy)(bpy)Ru^{II}(OH_2)]^{2+}$, is approximately octahedral with the ligating atoms being the three N atoms of the tpy ligand, the two N atoms of the bpy ligand, and the oxygen atom of the aqua ligand. The Ru-O bond length is 2.136(5) Å.

Introduction

Metal-oxo reagents such as $KMnO_4$ or $K_2Cr_2O_7$ are useful oxidants but difficult to control in terms of product distribution. The mechanisms of these reactions are hard to unravel because of the multiple oxidation states involved.[1]

A series of polypyridyl Ru and Os mono-oxo complexes are known, which have proved to be versatile stoichiometric and/or catalytic oxidants toward a variety of organic and inorganic substrates based on $Ru^{IV/III}$ and $Ru^{III/II}$ couples.[2] The cleavage of DNA has also been reported.[3] The results of mechanistic studies based on $[(bpy)_2(py)Ru^{IV}=O]^{2+}$ (bpy is 2,2′-bipyridine and py is pyridine) as oxidant with a variety of substrates have demonstrated many reaction pathways.[4] There is far less mechanistic information available for $[(tpy)(bpy)Ru^{IV}=O]^{2+}$ as oxidant even though it is of value in catalytic reactions.[5] Reduction potentials relating its three oxidation states at pH$=7$ (*vs* SSCE at 22 ± 2 ℃) are shown in the Latimer diagram in equation 1.

$$\underbrace{(tpy)(bpy)Ru^{IV}=O^{2+} \xrightarrow{0.62\ V} (tpy)(bpy)Ru^{III}\text{-}OH^{2+} \xrightarrow{0.49\ V} (tpy)(bpy)Ru^{II}OH_2^{2+}}_{0.56\ V} \quad (1)$$

In this manuscript we report on the kinetics and mechanisms of oxygenation of triphenylphosphine by $[(tpy)(bpy)Ru^{IV}(O)]^{2+}$ and the X-ray crystal structure of the parent complex $[(tpy)(bpy)Ru^{II}(OH_2)]^{2+}$.

Table 1. Crystal Data for $[(tpy)(bpy)Ru(OH_2)](ClO_4)_2$

formula	$RuC_{25}N_5O_9Cl_2H_{21}$
f(s), amu	707.5
System, Space group	Orthorhombic, Pbca
a, Å	10.854(12)
b, Å	32.738(7)
c, Å	15.349(4)
V, Å	5454
z	8
t, ℃	20
density (calcd), g/cm³	1.723
crystal shape, mm	0.14×0.05×1.27
radiation	Mo Kα (λ=0.7107) Zr-filtered
scan mode	$2\theta-\omega$
scan speed, deg/min	2
2θ limits, deg	$0<2\theta<50$
data collected	+h+k+l
P facter	0.02
No. of reflection measured	4017
No. of reflection used	2454
No. of variables	379
Collection	Lorentz-Polarization Extraction
R	0.079
Rw	0.057

Experimental Section

Materials. Triphenylphosphine was recrystallized twice from ethanol and checked by FT-IR to confirm the absence of the phosphine oxide ($\nu_{P=O}$) at 1194 cm^{-1} in a nujol mull.[6] Acetonitrile was purified by distillation from P_2O_5 under an Ar atmosphere. Water was purified by using a Nanopure™ (Barnstead) water system. ^{18}O-labeled water (isotope purity> 97.1%) was purchased from Isotec and used as received.

Preparations. $[(tpy)(bpy)Ru^{II}\text{-}OH_2](ClO_4)_2$, $[(tpy)(bpy)Ru^{II}\text{-}^{18}OH_2](ClO_4)_2$, $[(tpy)(bpy)Ru^{IV}=O](ClO_4)_2$, and $[(tpy)(bpy)Ru^{IV}={}^{18}O](ClO_4)_2$ were prepared by previously described procedures.[5c]

Instrumentation. Routine UV-visible spectra and slow kinetic runs were recorded on Hewlett-Packard 8452A diode array or Cary-14 spectrophotometers. FT-IR spectra were obtained on a Nicolet Mode 20DX FT-IR spectrophotometer as either nujol mull or in solution by using NaCl plates. Electrochemical measurements were conducted with a PAR Model 173 potentiostat/galvanostat connected to a PAR Model 175 universal programmer as a sweep generator for voltammetry experiments. The cyclic voltametric measurements utilized a Teflon-sheathed glassy-carbon disk (1.5 mm radius) as a working electrode, a platinum wire as the auxiliary electrode, and a saturated sodium chloride calomel reference electrode (SSCE) in a one-compartment cell. Fast kinetic measurements were carried out by using a Hi-Tech Scientific SF-51 stopped-flow apparatus with fiber-optic coupling to either Beckman DU or Harrick rapid scan monochromators. The system was interfaced to a Zenith 158 computer system employing On Line Instrument System (OLIS) data acquisition hardware and software (Jefferson, GA). All of the ^1H and ^{31}P NMR data were obtained with an IBM AC 200 spectrophometer or a Varian Gemini 200 MHz spectrometer by using CD_3CN as solvent. The chemical shift parameters were presented in parts per million (δ) downfield from tetramethylsilane (TMS) as an internal reference while the ^{31}P chemical shifts were referenced to external 85% H_3PO_4.

UV-visible measurements. The complex $[(tpy)(bpy)Ru^{II}\text{-}NCCH_3]^{2+}$ was prepared *in situ* by dissolving $[(tpy)(bpy)Ru^{II}\text{-}OH_2]^{2+}$ in CH_3CN.[7] Spectral changes with time showed that the half-life ($t_{1/2}$) of solvation was 15 min, $k=1.1\times10^{-3}$ s^{-1}.[8] The stoichiometry of the reaction between $[(tpy)(bpy)Ru^{IV}=O]^{2+}$ and PPh_3 in CH_3CN was determined in a spectrophometric titration where the Ru(IV) : PPh_3 mole ratio was varied beween 0 and 2 by adding different volumes of a stock solution of PPh_3 to equal volumes of a Ru(IV) stock solution and diluting each by 10 mL. No precautions were taken to exclude air.

Infrared measurements. 5 mg of freshly recrystallized PPh_3 in 10 mL of CH_3CN (1.9 mM) was added to 14 mg of solid $[(tpy)(bpy)Ru^{IV}(O)](ClO_4)_2$ (2.0 mM), and infrared spectra in a 1 mm pathlength NaCl cell were recorded at 1 min intervals in the region 1300-1050 cm^{-1}. After 1 day, infrared analysis for $OPPh_3$ based on $\nu(P=O)$ at 1194 cm^{-1} showed that free $O=PPh_3$ was formed quantitatively. $[(tpy)(bpy)Ru^{IV}(^{18}O)](ClO_4)_2$, containing an estimated 60% ^{18}O, was allowed to react with PPh_3 by the same procedure. As expected for O-atom transfer, both $\nu_{P={}^{16}O}$ (1194 cm^{-1}) and $\nu_{P={}^{18}O}$ (1161 cm^{-1}) were observed and in the expected ratio as shown by comparing the integrated intensities. Labeled product was shifted approximately 30 cm^{-1} to lower energy than the previously established standards.

Kinetic measurements. The oxidation of PPh_3 by Ru(IV) initially affords an intermediate with a λ_{max} at 485 nm. The rate of the reduction of Ru(IV) to this intermediate was followed by the absorbance changes against time at 468 nm. This wavelength is an isosbestic point for the intermediate and the final solvolysis product, $[(tpy)(bpy)Ru^{II}\text{-}NCCH_3]^{2+}$ ($\lambda_{max}=456$ nm). Stopped-flow measurements of the rate of formation of the intermediate were carried out on the Hi-Tech Scientific SF-51 stopped-flow apparatus under pseudo-first-order conditions with PPh_3 in excess. Reported values of the rate constants are averages of five or more experiments based on the same stock solutions.

X-ray crystallography. Brown black crystals were obtained from a saturated $NaClO_4$ solution containing $[(tpy)(bpy)Ru\text{-}OH_2]^{2+}$ by using slow evaporation. Cell constants, obtained at 293 K from least-squares refinement of 25 reflections on an Enraf-Nonius CAD 4 diffractometer equipped

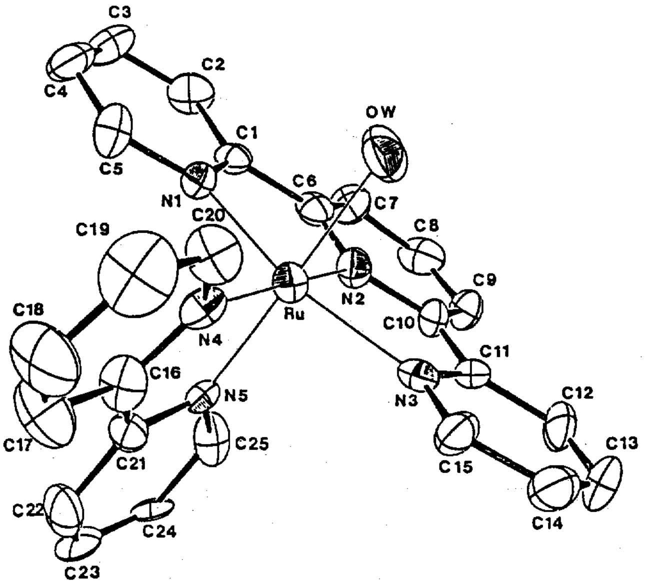

Figure 1. An ORTEP drawing of the [(tpy)(bpy)Ru(OH$_2$)]$^{2+}$ cation with the hydrogen atoms omitted for the sake of clarity.

Table 2. Principal Bond Distances (Å) in [(tpy)(bpy)Ru(OH$_2$)](ClO$_4$)$_2$[a]

bond	distance	bond	distance
Ru-OW	2.136(5)	C1-C2	1.38(1)
Ru-N1	2.053(6)	C1-C6	1.45(1)
Ru-N2	1.960(6)	C2-C3	1.41(1)
Ru-N3	2.062(7)	C3-C4	1.35(1)
Ru-N4	2.068(6)	C4-C5	1.39(1)
Ru-N5	2.015(6)	C6-C7	1.37(1)
C11-O11	1.361(8)	C7-C8	1.39(1)
C11-O12	1.361(7)	C8-C9	1.37(1)
C11-O13	1.407(7)	C9-C10	1.40(1)
C11-O14	1.400(7)	C10-C11	1.44(1)
C11-O21	1.356(9)	C11-C12	1.30(1)
C12-O22	1.33(1)	C12-C13	1.35(1)
C12-O23	1.25(1)	C13-C14	1.38(1)
C12-O24	1.354(9)	C14-C15	1.34(1)
N1-C1	1.376(9)	C16-C17	1.36(1)
N1-C5	1.38(1)	C16-C21	1.45(1)
N1-C6	1.345(9)	C17-C18	1.34(1)
N3-C10	1.35(1)	C18-C19	1.37(1)
N3-C11	1.35(1)	C19-C20	1.35(1)
N3-C15	1.32(1)	C21-C22	1.40(1)
N4-C16	1.35(1)	C22-C23	1.36(1)
N4-C20	1.32(1)	C23-C24	1.35(1)
N5-C21	1.34(1)	C24-C25	1.39(1)
N5-C25	1.35(1)		

[a] The numbering scheme is taken from Figure 1.

Table 3. Bond Angles (deg) in [(tpy)(bpy)Ru(OH$_2$)](ClO$_4$)$_2$[a]

bond	angle	bond	angle
OW-Ru-N1	88.5(2)	C1-C2-C3	10.6(9)
OW-Ru-N2	86.9(2)	C2-C3-C4	117.2(9)
OW-Ru-N3	87.4(2)	C3-C4-C5	122.1(9)
OW-Ru-N4	96.9(3)	N1-C5-C4	121.2(9)
OW-Ru-N5	174.9(3)	N2-C6-C1	114.3(7)
N1-Ru-N2	79.8(2)	C1-C6-C7	126.2(8)
N1-Ru-N3	158.7(3)	C6-C7-C8	118.3(9)
N1-Ru-N4	99.3(2)	C7-C8-C9	121.9(9)
N1-Ru-N5	93.2(2)	C8-C9-C10	118.4(8)
N2-Ru-N3	79.1(3)	N2-C10-C9	118.2(9)
N2-Ru-N4	176.1(3)	N2-C10-C11	112.7(9)
N2-Ru-N5	98.1(3)	C9-C10-C11	129.1(9)
N3-Ru-N4	102.0(3)	N3-C11-C10	116.5(8)
N3-Ru-N5	92.7(2)	N3-C11-C12	119.8(9)
N4-Ru-N5	78.1(3)	C11-C12-C13	119(1)
O111-C11-O12	110.8(6)	C12-C13-C14	120.3(9)
O11-C11-O13	113.2(6)	C13-C14-C15	116.3(9)
O11-C11-O14	110.0(6)	N3-C15-C14	125(1)
O12-C11-O13	109.1(4)	N4-C16-C17	121.0(9)
O12-C11-O14	108.1(6)	N4-C16-C21	114.3(8)
O13-C11-O14	105.4(5)	C17-C18-C19	118(1)
O21-C12-O22	111.9(9)	C18-C19-C20	119(1)
O21-C12-O23	104.2(8)	N4-C20-C19	123(1)
O21-C12-O24	113.1(7)	N2-C6-C7	119.5(8)
O22-C12-O23	109(1)	C10-C11-C12	123(1)
O22-C12-O24	102.6(7)	N5-C21-C16	114.9(9)
O23-C12-O24	115(1)	C17-C16-C21	124(1)
C1-N1-C5	117.6(7)	C16-C17-C18	120(1)
C6-N2-C10	123.6(8)	N5-C21-C22	119.1(9)
C11-N3-C15	118.3(8)	C21-C22-C23	121.5(9)
C16-N4-C20	117.8(8)	C22-C23-C24	119.9(9)
C21-N5-C25	118.4(8)	C16-C21-C22	126.0(9)
N1-C1-C2	121.3(8)	C23-C24-C25	117.1(9)
N1-C1-C6	114.6(7)	N5-C25-C24	123.9(8)
C2-C1-C6	124.1(8)		

[a] The numbering scheme is taken from Figure 1.

with a Mo tube and a Zr filter, are given in Table 1. The data were collected and reduced by previously described procedure.[9] The observed systematic absences of $h=2n+1$ for $hk0$, $k=2n+1$ for $hk0$, and $l=2n+1$ for $h0l$ uniquely define the space group as Pbca (No. 61).

The location of the ruthenium atom was determined by examination of a Patterson function, and the positions of all other atoms were located from subsequent difference Fourier maps. The locations of 19 of 21 hydrogen atoms in the structure were calculated on the basis of the geometries at the carbon atoms (C-H=0.95 Å). The two hydrogen atoms on the aqua ligand were found in a difference map, but attempts to refine these parameters were unsuccessful. Consequently, the final least-squares calculation included anisotropic refinement of the 42 atoms for a total of 379 variables and 2454 reflections.

A final difference Fourier map was featureless with no peak in excess of 0.33 e Å^{-3}. The atomic positional parameters (Table SI), the hydrogen atom positional parameters (Table SII), listings of thermal parameters (Table SIII), and structural amplitudes (Table SIV) are available as supple-

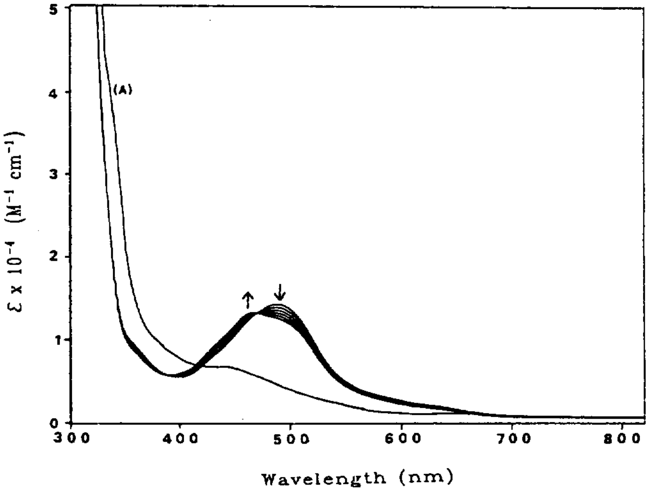

Figure 2. Succesive spectral changes taken at 1 min intervals after mixing PPh_3 (3×10^{-3} M) and $[(tpy)(bpy)Ru(O)]^{2+}$ (3×10^{-5} M) in CH_3CN. The initial spectrum of $[(tpy)(bpy)Ru(O)]^{2+}$ is shown as (A).

mental materials.

Results

Structure of $[(tpy)(bpy)Ru(OH_2)]^{2+}$. A perspective drawing of the complex with the numbering scheme of the atoms is shown in Figure 1.

The interatomic distances are presented in Table 2, and bond angles in Table 3. The ruthenium(II) center has approximately octahedral geometry. The three nitrogen atoms of terpyridine and one nitrogen atom (N4) of bipyridine are coordinated in the equatorial positions, while the other nitrogen (N5) of bipyridine and the oxygen atom of water are in the axial position. The three pyridine rings of terpyridine are nearly coplanar with no deviations from the plane larger than 0.19 Å The two pyridine rings of bipyridine are also coplanar (max. deviation=0.08 Å). These two planes are almost perpendicular, the interplanar angle being 87°. The only significant deviation from octahedral geometry at Ru is caused by the compression (to 158.7(3)°) of the *trans* N(1)-Ru-N(3) angle subtended by the nitrogen atoms of the terpyridine ligand.

There are two perchlorate anions in the asymmetrical unit. The thermal motion associated with two of the perchlorate oxygen atoms, O(22) and O(23), is very large, which might suggest the presence of some disorder. However no significant peaks could be found in a final difference Fourier.

UV-visible Spectral changes. The UV-visible spectral changes during the reaction of $[(tpy)(bpy)Ru(O)]^{2+}$ with PPh_3 in CH_3CN at room temperature are shown in Figure 2.

The initally featureless spectrum of $[(tpy)(bpy)Ru(O)]^{2+}$ (above 380 nm) changed rapidly to give a new species with $\lambda_{max}=485$ nm upon addition of PPh_3. The subsequent, far slower, spectral changes in Figure 2 are consistent with solvolysis of the initial intermediate by CH_3CN to yield $[(tpy)(bpy)Ru^{II}(NCCH_3)]^{2+}$ with $\lambda_{max}=456$ nm, equation 2.[7,10]

The spectrum of the intermediate is typical of other polypyridyl complexes of Ru(II) and consists of metal-to-ligand-charge transfer (MLCT) bands between Ru(II) and both tpy and bpy as acceptor ligands. For example, for $[(tpy)(bpy)Ru^{II}\text{-}OH_2]^{2+}$ in H_2O, $\lambda_{max}=456$ nm[5] and for $[(bpy)_2(py)Ru(OPPh_3)]^{2+}$ in CH_3CN, $\lambda_{max}=479$ nm.[7]

Product Analysis and Stoichiometry. The reaction between $[(tpy)(bpy)Ru^{IV}(O)]^{2+}$ and PPh_3 was investigated by spectrophotometric titration. With the addition of PPh_3, the visible absorption maximum at 456 nm for $[(tpy)(bpy)Ru^{II}\text{-}NCCH_3]^{2+}$ increases until a mole ratio (PPh_3/Ru) of 1 : 1 was reached past which there were no further changes. The measurements at 456 nm were made after sovolysis of the triphenylphosphine oxide complex had occurred. A blank solution of Ru(IV) without added PPh_3 in CH_3CN was stable over the timescale of the experiment. The free $O=PPh_3$ obtained after precipitation of ruthenium complex was quantitative to PPh_3.

$$[(tpy)(bpy)Ru^{IV}=O]^{2+}+PPh_3 \xrightarrow{CH_3CN} [(tpy)(bpy)Ru^{II}\text{-}NCCH_3]^{2+}+O=PPh_3 \qquad (2)$$

The reaction was also followed by FT-IR. Shortly after mixing 5 mg of triphenylphosphine (19 mM) with 14 mg of $[(tpy)(bpy)Ru^{IV}=O]^{2+}$ (20 mM) in 1 mL of CH_3CN, ν(P=O) appeared at 1161 cm^{-1}.[11] Over the period of slow solvolysis in Figure 2, the band at 1161 cm^{-1} decreased in intensity while the 1194 cm^{-1} peak of free $OPPh_3$ increased. The decrease in ν(P=O) for bound $OPPh_3$ is consistent with O-bound triphenylphosphine oxide.[11]

The reaction was also followed by ^{31}P and ^{1}H NMR in the bipyridine region. For a reaction mixture consisting of 19 mM of $[(tpy)(bpy)Ru^{IV}(O)]^{2+}$ and 20 mM of PPh_3 in 1 mL of CD_3CN, changes in the 6′ proton resonance of bipyridine from 9.2 to 10.0 ppm were followed with time. Shortly after mixing, resonances at 9.75 ppm and 9.60 ppm were present. After 4 h, the resonance at 9.75 ppm decreased in intensity with concommitant increase in the resonance at 9.60 ppm, which by independendent measurement, corresponds to $[(tpy)(bpy)Ru^{II}\text{-}NCCD_3]^{2+}$. After 16 h, only the resonance at 9.60 ppm was detected.

In a solution formed by mixing 7 mg of PPh_3 (2.8 mM) and 14 mg of $[(tpy)(bpy)Ru(O)]^{2+}$ (2.0 mM) in 10 mL of CH_3CN, ^{31}P resonances appeared at −4.5 ppm for PPh_3 and a second at 49.5 ppm arising from the intermediate. After 1 h, the resonance at 49.5 ppm had decreased with simultaneous increase in the 27.4 ppm resonance for $O=PPh_3$. When the reaction was complete, only the resonance at 27.4 ppm was observed.

Kinetics. The rate of the formation of the intermediate in CH_3CN was studied by monitoring absorbance-time traces at 468 nm by stopped-flow. Under pseudo-first-order conditions with PPh_3 in excess, the kinetics of formation of $[(tpy)(bpy)Ru^{II}\text{-}OPPh_3]^{2+}$ were cleanly first order in $[PPh_3]$. The kinetics data are summarized in Table 4. At 25.3 ℃, $k=1.25\times10^{6}$ $M^{-1}s^{-1}$ was averaged over five concentrations of PPh_3 in pseudo-first-order excess. From rate constant measurements as a function of temperature and plots of $\ln(k/T)$ *vs* $1/T$ according to reaction rate theory,[12] $\Delta H^{\neq}=3.5\pm0.5$ kcal/mol and $\Delta S^{\neq}=-23\pm3$ eu. For solvolysis of $[(tpy)(bpy)Ru^{II}(OPPh_3)]^{2+}$ in CH_3CN at 25.3 ℃, $t_{1/2}=250$ min ($k=6.7\times10^{-5}$ s^{-1}) as an average of five kinetic runs.

Table 4. Kinetic Data for the Initial Redox Reaction between Triphenylphosphine and $[(tpy)(bpy)Ru^{IV}=O]^{2+}$ IN CH_3CN

$10^5\times[Ru(IV)]$, M	$10^4\times[PPh_3]$, M	$10^{-6}\times k^a$, $M^{-1}S^{-1}$	T, ℃
1.52	2.04	0.92 ± 0.01	15.7
1.52	4.07	0.97 ± 0.04	15.8
1.62	2.07	1.17 ± 0.03	25.1
1.62	3.10	1.25 ± 0.05	25.3
1.62	4.14	1.29 ± 0.08	25.4
1.68	1.53	1.44 ± 0.07	33.8
1.68	2.04	1.48 ± 0.06	33.8
1.68	4.07	1.52 ± 0.10	33.9
1.86	1.53	1.68 ± 0.02	39.7
1.86	3.05	1.67 ± 0.04	39.7

[a] Each rate constant is the average of four or more experimental results. Second- order rate constants were caculated from $k_{obs}/[PPh_3]$ under pseudo-first-order condition in excess PPh_3 where k_{obs} is the pseudo-first-order rate constant.

Labeling Studies. The oxidant $[(tpy)(bpy)Ru(O)]^{2+}$ containing 60 atom % of $[Ru(^{18}O)]^{2+}$ was allowed to react with PPh_3 in CH_3CN, and the product solution analyzed by FT-IR spectrophotometer. Quantitative analysis of $^{18}OPPh_3$ (1161 cm^{-1}) and $OPPh_3$ (1194 cm^{-1}) showed essentially complete oxygen transfer from $[(tpy)(bpy)Ru^{IV}=O]^{2+}$ to PPh_3.[8] A test for trace water as the oxygen source was made by allowing unlabeled $Ru^{IV}=O^{2+}$ and PPh_3 to react in CH_3CN including 1 drop of $^{18}OH_2$ (95% ^{18}O). This showed that less than 5% of the $OPPh_3$ formed had incorporated the label. The small degree of ^{18}O incorporation probably comes from exchange between $[(tpy)(bpy)Ru^{IV}=O]^{2+}$ and H_2O.[7]

Electrochemical Measurements. Although reduction of $[(tpy)(bpy)Ru^{IV}(O)]^{2+}$ to $[(tpy)(bpy)Ru^{III}(O)]^{+}$ is chemically irreversible, it can be estimated that $E_{1/2}$ is less than 0.1 V *vs* SSCE. For the $PPh_3^{0/+}$ couple, oxidation of PPh_3 is also chemically irreversible with $E_{1/2}>1.32$ V *vs*. SSCE under the same conditions.[7]

Discussion

From the spectroscopic observations, the mechanism of oxygenation of PPh_3 by $[(tpy)(bpy)Ru^{IV}(O)]^{2+}$ involves a fast 2 electron transfer to give bound $OPPh_3$ in $[(tpy)(bpy)Ru^{II}\text{-}OPPh_3]^{2+}$ followed by a far slower solvolysis,

$$[(tpy)(bpy)Ru^{IV}=O]^{2+}+PPh_3 \xrightarrow{k(25\ ℃)=1.25\times10^6\ M^{-1}s^{-1}}$$

$$[(tpy)(bpy)Ru^{II}\text{-}OPPh_3]^{2+}$$

$$\downarrow k(25\ ℃)=6.7\times10^{-5}\ s^{-1}$$

$$[(tpy)(bpy)Ru^{II}\text{-}NCCH_3]^{2+}+OPPh_3 \quad (3)$$

This mechanism is consistent with the result of the ^{18}O-isotopic labeling study which shows that net oxygen atom transfer from $Ru^{IV}=O^{2+}$ to PPh_3 occurs and with the mechanism established for the reaction between PPh_3 and $[(bpy)_2(py)Ru^{IV}(O)]^{2+}$ in CH_3CN.[13]

There are serveral mechanistic possibilities for the initial redox step which have been discussed elsewhere.[13] Initial outer-sphere electron transfer is not feasible on energetic grounds. By combining the two $E_{1/2}$ estimates for the $[(tpy)(bpy)Ru(O)]^{2+/+}$ and $PPh_3^{0/+}$ couples, initial one electron transfer may be nonspontaneous by more than 1.0 eV. Amongst other mechanisms that have been mentioned is prior nucleophilic attack of PPh_3 on Ru(IV) followed by migration of the coordinated phosphorous to the oxo group.[15] Although seven-coordinate complexes of Ru(IV) are known,[16] the formation of a seven-coordinate phosphine complex in this coordination environment seems unlikely based on steric considerations as predicted both by molecular models and related coordination chemistry.[17]

Table 5. Comparison of Ru-O Bond Distances (Å) with Related Complexes

Complex	Ru-O	length (Å)	ref
$[Ru(tpy)(bpy)(OH_2)](ClO_4)_2$	Ru(II)-OH_2	2.130	this work
$[Ru(H_2O)_6](C_7H_7SO_3)_2$	Ru(II)-OH_2	2.122	20
$[Ru(H_2O)_6](C_7H_7SO_3)_3\cdot3H_2O$	Ru(III)-OH_2	2.049	20
$[Ru(OH)Cl(py)_4]^+$	Ru(III)-OH	1.957	21
$[RuCl(O)(py)_4]^+$	Ru(IV)-O	1.862	22
$[Ru(TMC)(O)(MeCN)]^{2+}$	Ru(IV)-O	1.765	13
(TMC = 1,4,8,11-tetramethyl-1,4,8,11-tetraazacyclotetradecane)			

The most likely mechanism is a concerted O-atom transfer from $Ru^{IV}=O^{2+}$ to PPh_3. In this reaction the acceptor orbitals are the π antibonding orbitals of the Ru-oxo group which are largely $d\pi$(Ru) in character.[18,19] With electron flow to Ru, largely O-based electron density is made available for the O-P bonding interaction.

Quantitative comparison between the reactivities of the tpy-bpy and bis/bpy-py oxo complexes toward oxidation of PPh_3 shows that the rate constant for the former is about 7 times faster than the latter $[Ru(bpy)_2(py)(O)]^{2+}$, 1.75×10^5 $M^{-1}s^{-1}$ (26.5 ℃); $[Ru(tpy)(bpy)(O)]^{2+}$, 1.25×10^6 $M^{-1}s^{-1}$ (25.3 ℃). The difference in rate constants occurs in ΔH^* ($[Ru^{IV}(bpy)_2(py)(O)]^{2+}$, 4.7 kcal/mol; $[Ru^{IV}(tpy)(bpy)(O)]^{2+}$, 3.4 kcal/mol). The ΔS^* values are the same within experimental error (-19 ± 3 eu for $[Ru^{IV}(bpy)_2(py)(O)]^{2+}$ compared to -23 ± 3 eu for $[Ru^{IV}(tpy)(bpy)(O)]^{2+}$), consistent with a common mechanism. The higher rate constant for $[(tpy)(bpy)Ru(O)]^{2+}$ reflects its higher driving force as an oxidant. The potential for the 2-electron $Ru^{IV}=O^{2+}/Ru^{II}\text{-}OH_2^{2+}$ couples are 0.56 V (Equation 1) and 0.47 V *vs* SSCE at pH 7. The solvolysis rate constant for $[(tpy)(bpy)Ru^{II}\text{-}OPPh_3]^{2+}$, $k(25\ ℃)=6.7\times10^{-5}\ s^{-1}$ is slower than for $[(bpy)_2(py)Ru^{II}\text{-}OPPh_3]^{2+}$, $k(25\ ℃)=1.5\times10^{-4}\ s^{-1}$. As in other complexes of this kind, substitution rates tend to decrease as the $Ru^{III/II}$ potential increases. Both respond to increasing stabilization of d electrons by ligand field effects.

In $[(tpy)(bpy)Ru\text{-}OH_2]^{2+}$, the Ru-$OH_2$ bond distance of 2.136(6) Å, is consistent with the expected Ru-O single bond. For comparison, Ru-O bond distances for other complexes of Ru(II), Ru(III), and Ru(IV) are listed in Table 5.

Some of the spectroscopic results that were acquired provide insight into various aspects of the coordination chemistry. In complexes of the type $[(tpy)(bpy)Ru^{II}(L)]^{2+}$, the 6′-proton of the bipyridine ring that is near ligand L, Figure 1, is shifted relatively further downfield compared to the remaining bipyridine protons.[18] Based on the numbering scheme in Figure 1, the 6′-proton, which is on C20, exists out of the ring current of the aromatic terpyridine ligand and towards the sixth non-pyridyl ligand. This resonance provides a characteristic marker for the sixth ligand. For the O-bound triphenylphosphine oxide complex, the doublet for the 6′-proton appears at 9.75 ppm and for the CD_3CN complex at 9.60 ppm.

The ^{31}P NMR resonance for $[(tpy)(bpy)Ru\text{-}OPPh_3]^{2+}$ is at 49.5 ppm, for PPh_3 at -4.5 ppm, and for $O=PPh_3$ at 27.4 ppm.[23] The shift in the resonance between free and bound $OPPh_3$ reflects the depletion of electron density on the phosphorous atom by coordination to ruthenium.

The $\nu(P=O)$ band for free triphenylphosphine oxide at 1194 cm^{-1} is shifted by *ca.* 42 ± 6 cm^{-1} to lower energy when coordinated to a metal.[11a] The shift in $\nu(P=O)$ for $[(tpy)(bpy)Ru^{II}\text{-}OPPh_3]^{2+}$ is 33 cm^{-1} suggesting a greater degree of $P=O$ double bond character in the complex.

Acknowledgment. are made to the Korea Science and Engineering Foundation (to Won K. Seok) and the National Science Foundation under Grant No. CHE-9203311 for support of this research.

References

1. (a) Mijs, W. J.; De Jonge, C. R. H. I. *Organic Syntheses by Oxidation with Metal Compounds*; Plenum Press: New York, 1986. (b) Holm, R. H. *Chem. Rev.* **1987**, *87*, 1401.
2. (a) Leising, R. A.; Kubow, S. A.; Churchill, M. R.; Buttrey, L. A.; Ziller, J. W.; Takeuchi, K. J. *Inorg. Chem.* **1990**, *29*, 1306. (b) Che, C. M.; Leung, W. H.; Chung, W. C. *Inorg. Chem.* **1990**, *29*, 1841. (c) Bruice, T. C. *Acc. Chem. Res.* **1991**, *24*, 243. (d) Binstead, R. A.; McGuire, M. E.; Dovletoglou, A.; Seok, W. K.; Roecker, L. E.; Meyer, T. J. *J. Am. Chem. Soc.* **1992**, *114*, 173. (e) Griffth, W. P. *Chem. Soc. Rev.* **1992**, 179.
3. (a) Kalsbeck, W. A.; Thorp, H. H. *Inorg. Chem.* **1994**, *33*, 3417. (b) Meunier, B. *Chem. Rev.* **1992**, *92*, 1411.
4. Dovletoglou, A.; Meyer, T. J. *J. Am. Chem. Soc.* **1994**, *116*, 215 and references cited therein.
5. (a) Moyer, B. A.; Thompson, M. S.; Meyer, T. J. *J. Am. Chem. Soc.* **1980**, *102*, 2310. (b) Samuels, G. J.; Meyer, T. J. *J. Am. Chem. Soc.* **1981**, *103*, 307. (c) Thompson, M. S. Ph.D Dissertation, The Univ. of North Carolina, Chapel Hill, NC, 1981. (d) Thompson, M. S.; De Giovani, W. F.; Moyer, B. A.; Meyer, T. J. *J. Org. Chem.* **1984**, *49*, 4972.
6. Halmann, M.; Pinchas, S. *J. Chem. Soc.* **1958**, 3264.
7. (a) Moyer, B. A.; Sipe, B. K.; Meyer, T. J. *Inorg. Chem.* **1981**, *20*, 1475. (b) Roecker, L. E.; Dobson, J. C.; Vining, W. J.; Meyer, T. J. *Inorg. Chem.* **1987**, *26*, 779.
8. Unpublished results from Seok, W. K.
9. Graves, B. J.; Hodgson, D. J. *Acta Cryst.* **1982**, *B38*, 135.
10. Seok, W. K. *Bull. Korean Chem. Soc.* **1993**, *14*, 433.
11. (a) Cotton, F. A.; Barnes, R. D.; Bannister, E. *J. Chem. Soc.* **1960**, 2199. (b) Nakamoto, K. *Infrared Spectra of Inorganic and Coordination Compounds*; 2nd ed.: Wiley; New York, 1970.
12. Moore, J. W.; Pearson, R. G. *Kinetics and Mechanism*; 3r ed.; Wiley: New York, 1981.
13. (a) Che, C. M.; Wong, K. Y.; Mak, T. C. W. *J. Chem. Soc., Chem. Commun.* **1985**, 546. (b) Marmion, M. E.; Takeuchi, K. J. *J. Am. Chem. Soc.* **1986**, *108*, 510. (c) Lau, T. C.; Kochi, J. K. *J. Chem. Soc., Chem. Commun.* **1987**, 179.
14. Latimer, W. M. *Oxidation Potentials*; 2nd ed.: Prentice Hall, Inc.; Englewood Cliffs, N. J. 1952.
15. Barral, R.; Bocard, C.; Seree de Roch, I.; Sajas, L. *Tetrahedron Lett.* **1972**, 1693.
16. Given, K. W.; Mattson, B. M.; Pignolet, L. H. *Inorg. Chem.* **1976**, *15*, 3152. (b) Mattson, B. M.; Pignolet, L. H. *Inorg. Chem.* **1977**, *16*, 488.
17. Meyer, T. J.; Salmon, D. J.; Sullivan, B. P. *Inorg. Chem.* **1978**, *17*, 3334.
18. Dobson, J. C.; Helms, J. H.; Doppelt, P.; Sullivan, B. P.; Hatfield, W. E.; Meyer, T. J. *Inorg. Chem.* **1989**, *28*, 2200.
19. Cundari, T. R.; Drago, R. S. *Inorg. Chem.* **1990**, *29*, 487.
20. Bernbard, P.; Burgi, H.; Hauser, J.; Lehman, H.; Ludi, A. *Inorg. Chem.* **1982**, *21*, 3936.
21. Aoyagi, K.; Nagao, H.; Yukawa, Y.; Ogura, M.; Kuwayama, A.; Howell, S.; M. Mukaida, Kakihana, H. *Chem. Lett.* **1986**, 2136.
22. Aoyagi, K.; Yukawa, Y.; Shimizu, K.; Mukaida, M.; Takeuchi, T.; Kakihana, H. *Bull. Chem. Soc. Jpn.* **1986**, *59*, 1493.
23. Gorestein, D. G. Ed. *^{31}P NMR, Principles and Applications*; Academic Press: N. Y., 1984.